Chin. J. Astron. Astrophys. Vol. 7 (2007), No. 5, 620–628
(*http://www.chjaa.org*)

Chinese Journal of
Astronomy and
Astrophysics

Luminosity Function of the Cluster of Galaxies Abell 566 *

Quan-Bao Xiao[1,2], Zheng-Yi Shao[1,2] and Xu Zhou[3]

[1] Shanghai Astronomical Observatory, Chinese Academy of Sciences, Shanghai 200030
zyshao@shao.ac.cn
[2] Joint Institute for Galaxy & Cosmology, Chinese Academy of Sciences, Shanghai 200030
[3] National Astronomical Observatories, Chinese Academy of Sciences, Beijing 100012

Received 2006 December 18; accepted 2007 April 28

Abstract We investigate the Luminosity Function (LF) of the cluster of galaxies Abell 566. The photometric data of 15 intermediate-bands are obtained from the Beijing-Arizona-Taiwan-Connecticut (BATC) photometric sky survey. For each of the 15 wavebands, the LF of cluster galaxies is well modelled by the Schechter function, with characteristic luminosities from –18.0 to –21.9 magnitude, from the a- to the p-band. Morphological dependence of the LF is investigated by separating the cluster members into 'red' and 'blue' subsamples. It is clear that late type galaxies have a steeper shape of LF than the early type galaxies. We also divided the sample galaxies by their local environment. It was found that galaxies in the sparser region have steeper shape of LF than galaxies in the denser region. Combining the results of morphological and environmental dependence of LFs, we show that Abell 566 is a well relaxed cluster with positive evidence of galaxy interaction and merger, and excess number of bright early type galaxies located in its denser region.

Key words: galaxy: cluster: individual: Abell 566 — galaxy: photometry — galaxy: luminosity function

1 INTRODUCTION

The galaxy luminosity function (LF) describes the luminosity distribution of galaxies. It is a fundamental measurement of galaxy formation and evolution, further acts as a powerful tool to investigate the properties of galaxies in a cluster. Schechter (1976) proposed an analytic expression for the LF, now well known as the Schechter function. The LF expressed per unit magnitude is

$$\phi(M)dM = \phi^* 10^{-0.4(M-M^*)(\alpha+1)} \exp[-10^{-0.4(M-M^*)}]dM, \quad (1)$$

where ϕ^* is a normalization coefficient, α is the logarithmic slope of $\phi(M)$ at the faint end and M^* is the characteristic magnitude, which is sometimes called "the knee" magnitude that separates the exponential and power law parts of $\phi(M)$.

Schechter suggested that the shape of LF of galaxy cluster is universal (with $\alpha \simeq -1.25$) and only ϕ^* differs among clusters. This universal LF hypothesis has been tested and argued by many authors. For example, Lugger (1986), Colless (1989), Lumsden et al. (1997), Trentham (1998) and Rauzy et al. (1998) supported the universal hypothesis, but Dressler (1978), Valotto et al. (1997) and Lopez-Cruz et al. (1997) etc., argued against it.

As a matter of fact, it has been found that the LF is dependent on the galaxy types and the environment. For example, Sandage, Binggeli & Tammann (1985) studied the LF of galaxies of various Hubble types in

∗ Supported by the National Natural Science Foundation of China.

the Virgo Cluster. They constructed the type specific luminosity function (TSLF) for each morphological type, and declared that E, S0 and all of spiral types have a TSLF close to a Gaussian, while dwarf ellipticals have an exponential TSLF. Subsequently, other authors (e.g. Andreon et al. 1997; Jerjen & Tamman 1997; Andreon 1998) supported such a suggestion by comparing the TSLFs measured in different environments. However, this conclusion is controversial. Some authors (e.g. Valotto et al. 1997; Bromley et al. 1998; Ramella et al. 1999 and Marinoni et al. 1999) found that instead of the significant differences in TSLF, various environments also affect the LF, and they claimed that, in general, the LF must be expressed as a function of both density and morphology: $\phi(T, \rho)$. This result could be explained by the morphology-density relation (Dressler 1980): since the morphology T is related to the density ρ or the environment, it is certain that LFs depend on both of them.

Abell 566, located at (106.1245°, 63.2921°) $_{\rm J2000}$, is a young nearby rich galaxy cluster with $z = 0.09730$ (Struble et al. 1999). It is one of the targets of the multi-color survey project of Beijing-Arizona-Taipei-Connecticut (BATC). Zhou et al. (2003) reported the data reduction of this cluster in detail. They collected 561 member galaxies of this cluster based on the photometric redshift. In this paper, we investigate the multi-band LFs of this cluster. Then, by using the relation between the BATC and $UBVRI$ broadband photometric systems, we also estimate the LFs of these broad bands and compare them with previous studies. Additionally, since the sample of member galaxies is adequate to be separated into two subsamples by either color or local density, their morphological and environmental dependence are studied as well.

This paper is organized as follows: in Section 2, we introduce the photometric data on 15 BATC filters and transfer them to the broadband system. The fitting methods (maximum-likelihood) and results of LF for multiple bands are shown in Section 3, while the morphological and environmental dependent LFs are discussed in Section 4. Conclusions are summarized in Section 5. We use the standard $\Lambda-$ cosmology with $\Omega_0 = 0.3$, $\Omega_\Lambda = 0.7$ and $H_0 = 100\,h{\rm km\,s^{-1}\,Mpc^{-1}}$ with $h = 1$.

2 DATE REDUCTION

The BATC photometric system, which comprises 15 intermediate bands and covers the range of optical wavelengths from 300 to 1000 nm (Fan et al. 1996; Zhou et al. 2001), is a large field multi-color photometric system. The field of view of the CCD is $58' \times 58'$ with a plate scale of 1.7 arcsec per pixel. The BATC magnitudes are defined in the AB_ν system of Oke & Gunn (1983).

From March 1995 to January 2002, the BATC survey project observed Abell 566 in 15 bands for more than 85 hours. The bias subtraction and dome flat-field correction were done by an automatic data reduction procedure called 'Pipeline 1' (Fan et al. 1996). Another software, 'Pipeline 2', was used to deal with the source photometry. To calibrate the flux, four standard stars, BD+17 °4708, BD+26°2606, HD19445 and HD84937 of Oke & Gunn(1983), were used. The details of the data reduction of Abell 566 can be found in Zhou et al. (2003).

Redshift is an important parameter for separating cluster members from field galaxies. Since the BATC intermediate bands cover almost the whole range of optical waveband, it was possible to derive the photometric redshifts of the individual galaxies. Zhou et al. (2003) listed the photometric redshifts with errors ($\sim$0.03) for all extend sources in this field, and selected 561 cluster member galaxies, whose photometric redshifts are within the range of [0.05, 0.15]. In this paper, we use their membership result directly in constructing the LF of Abell 566.

Furthermore, to correct the Galactic dust extinction, we use the procedure package of Schelegel et al. (1998) to extract the $V-$band extinction, A_V. Since the cluster galaxies are all located in a small region in the sky (less than one degree), their extinction values are all similar, with a typical value of $A_V = 0.17$. Then, to obtain the particular extinction values for the BATC wavebands, we adopted the extinction law of O'Donnell et al. (1994). In the optical, the relation between the extinctions in the $V-$band and other bands can be represented by a function $A_\lambda/A_V = a(x) + b(y)/3.1$, with

$$a(x) = 1 + 0.104y - 0.609y^2 + 0.701y^3 + 1.137y^4 - 1.718y^5 - 0.827y^6 + 1.647y^7 - 0.505y^8\,, \quad (2)$$

$$b(x) = 1.952y + 2.908y^2 - 3.989y^3 - 7.985y^4 + 11.102y^5 + 5.491y^6 - 10.805y^7 + 3.347y^8\,, \quad (3)$$

where $y = x - 1.82\mu{\rm m}^{-1}$ and $x = 1/\lambda(\mu{\rm m})$. Using this method, we calculate Galactic extinction A_λ in each band for all the sample galaxies. As a result the absolute magnitude was found according to

$$M_\lambda = m_\lambda - 5\log(d_{\rm L}/10\,{\rm pc}) - A_\lambda\,, \quad (4)$$

where m_λ is the apparent magnitude of BATC, $d_{\rm L}$ is the luminosity distance. In this work, $d_{\rm L}$ equals $313.2\,{\rm Mpc}$.

Through a comparison of 48 stars in the field of Landolt SA95 (Landolt 1983), Zhou et al. (2003) derived the correlations between the BATC intermediate-band system and the $UBVRI$ broadband system:

$$m_U = m_b + 0.6801(m_a - m_b) - 0.8982 \pm 0.143\,, \quad (5)$$

$$m_B = m_d + 0.2201(m_c - m_e) + 0.1278 \pm 0.076\,, \quad (6)$$

$$m_V = m_g + 0.3292(m_f - m_h) + 0.0476 \pm 0.027\,, \quad (7)$$

$$m_R = m_i + 0.1036 \pm 0.055\,, \quad (8)$$

$$m_I = m_o + 0.7190(m_n - m_p) - 0.2994 \pm 0.064\,. \quad (9)$$

So, we can apply these equations to convert the BATC magnitudes to the $UBVRI$ system, then it will be easy to make direct comparison with results of other clusters.

We note that it is difficult to examine the completeness of the sample, because Abell 566 is a rather distant target. So, we adopted a simple method to work out the flux limitation of cluster galaxies for each band. First, the magnitude range from –22 to –18 is split into bins of 0.2 magnitude width, then, the bin with the largest number of galaxies is chosen to define the magnitude limit: we simply regard the member galaxies are complete to this magnitude. The completeness magnitudes for the different bands are listed in Table 1.

Table 1 Luminosity Function Parameters of 15 Intermediate Bands of BATC and 5 Board Bands

Filter	N_g	Flux limits	α	M^*	$M_1^*(\alpha=-1.25)$	ϕ^*
a	194	–18.80	–0.08±0.33	–17.29±0.13	–18.01±0.24	133.10
b	331	–18.60	–0.39±0.11	–18.14±0.12	–19.15±0.25	108.63
c	328	–19.00	–0.44±0.15	–18.45±0.13	–19.41±0.29	114.45
d	355	–19.40	–0.98±0.13	–19.56±0.19	–20.03±0.29	71.17
e	370	–19.60	–0.86±0.11	–19.67±0.15	–20.26±0.31	81.31
f	282	–20.20	–1.28±0.14	–20.34±0.24	–20.3±0.29	47.66
g	411	–19.80	–1.06±0.11	–20.39±0.17	–20.71±0.26	57.89
h	345	–20.20	–1.39±0.10	–21.04±0.25	–20.78±0.21	30.25
i	308	–20.50	–1.26±0.13	–20.97±0.23	–20.95±0.22	40.40
j	294	–20.60	–1.32±0.13	–21.27±0.25	–21.15±0.23	31.42
k	285	–20.80	–1.35±0.10	–21.47±0.32	–21.29±0.28	29.72
m	267	–21.00	–1.26±0.15	–21.37±0.25	–21.36±0.26	37.88
n	394	–20.40	–1.19±0.12	–21.42±0.21	–21.55±0.23	37.95
o	410	–20.40	–1.21±0.09	–21.70±0.24	–21.79±0.24	33.04
p	349	–20.80	–1.41±0.20	–22.32±0.38	–21.87±0.25	18.74
U	238	–19.60	–0.67±0.22	–18.75 ±0.15	–19.28 ±0.24	108.57
B	332	–19.20	–0.83±0.14	–19.04 ±0.17	–19.62 ±0.25	86.90
V	380	–19.80	–1.10±0.11	–20.28 ±0.19	–20.53 ±0.24	55.77
R	308	–20.40	–1.28±0.13	–20.89 ±0.23	–20.87 ±0.22	39.02
I	371	–20.80	–1.02±0.11	–21.38 ±0 .18	–21.77 ±0.22	54.26

3 LUMINOSITY FUNCTION

3.1 The LFs of BATC Intermediate-bands

Using all the member galaxies brighter than the completeness magnitude, we constructed the LF of the galaxies in Abell 566 for each waveband. We use the maximum likelihood approach (Sandage et al. 1979, hereafter STY) to estimate the shape parameters of Schechter function, α and M^* (Eq. (1)), and normalize ϕ^* by using the number of galaxies within the range from the completeness magnitude to that of the third brightest galaxy.

Figure 1 shows the best fit Schechter function for all the intermediate bands by using the STY method. The dots with error bars denote the number counts and their Poisson errors. The fitting parameters are listed

in Table 1. It is clear that the Schechter function can model the luminosity distribution quite well for all the bands. However, the exposure of this cluster is still not deep enough, and for all BATC wavebands the complete sample covers a range of less than three magnitudes, so there is only a short range of the faint part of the LF (fainter than the M^*) included in the complete sample, especially for the bluer bands. Since the slope parameter α mainly describes the shape of the LF at the faint end, our sample is not good enough to constrain the value of α. As one can see in Table 1, α varies greatly among the different bands. For the redder bands, the values of α are similar to the 'universal LF' (≈ -1.25, Schechter 1976), while for the bluer bands, they are greater than –1.0. It is mainly due to the brighter flux limitation that fewer faint galaxies are included in the complete sample. Anyway, in order to compare the LFs of all bands, we additionally fitted the LFs with the Schechter function with a fixed $\alpha = -1.25$, which seems to be an acceptable value. These fitting results are also plotted in Figure 1 (shown as dashed lines), and the M^*s are listed in Table 1. It may be seen that, for galaxies brighter than M^*, the shape of LF is not sensitive to α.

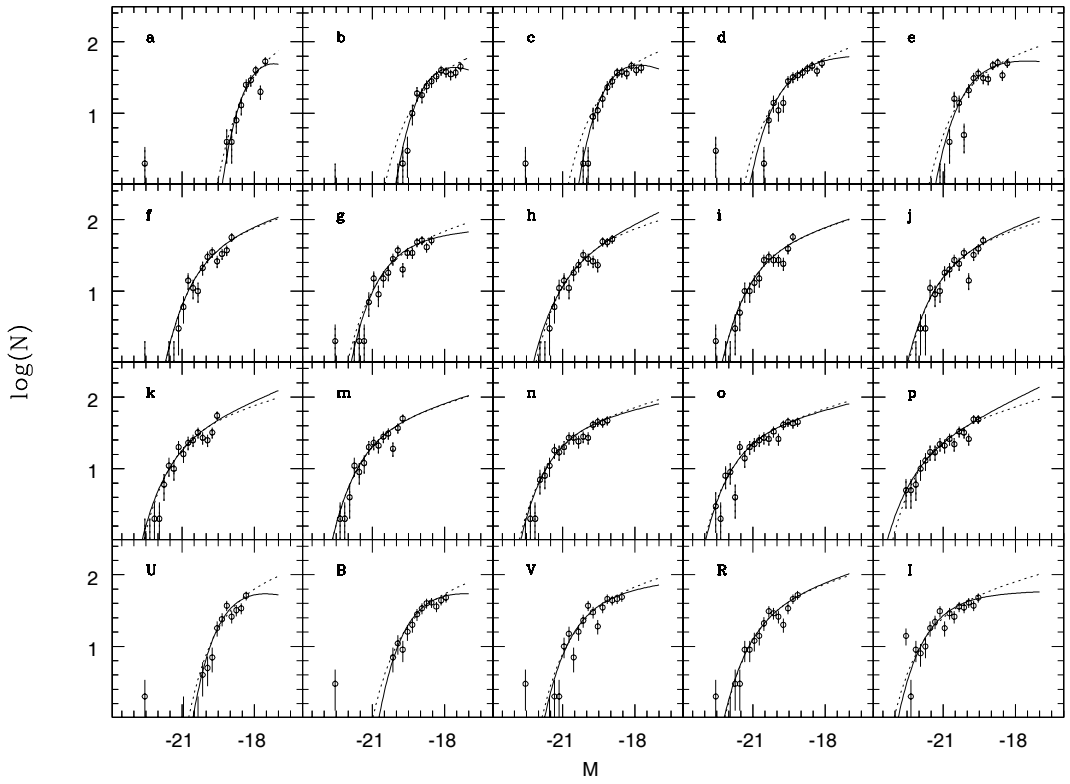

Fig. 1 LFs for all 15 intermediate bands of BATC and 5 board bands. The dots with error bars are galaxy counts, solid lines are the Schechter function of the best fit and dashed lines are the LFs with fixed $\alpha = -1.25$.

In Figure 2 we plot in order all the M^*s of the various bands. It could be regarded as the SED of the cluster. We note in this plot that the M^* sequence with fixed value of α is smoother than the original one with α adjustable.

3.2 The LFs of Broadbands

Using Equations (5)–(9), we convert the BATC magnitudes to the broadband magnitudes, U, B, V, R, I. For each band, we define a completeness magnitude as before, and construct the individual LFs. Just as shown in Figure 1 (the bottom panel), for each band the luminosity distribution of member galaxies is also in good agreement with the Schechter function. The fitting parameters are given in Table 2.

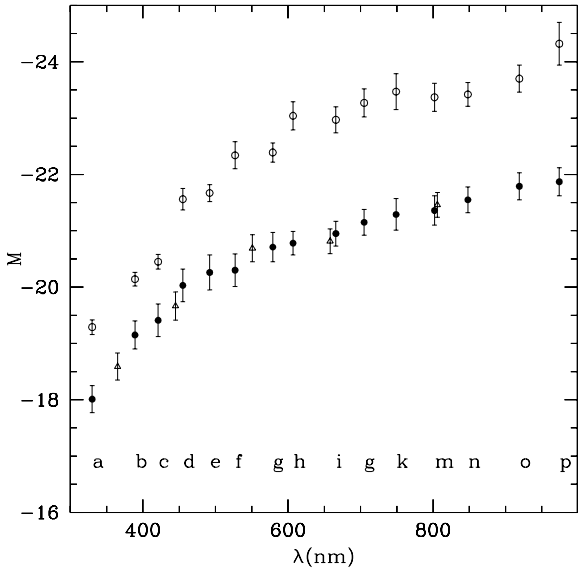

Fig. 2 M^* sequence along the various wavebands. Open circles are best fitting values of M^*, artificially shift 2 magnitude towards the brighter end, in order to avoid the confusion with other points. Filled circles are M^*s with fixed $\alpha = -1.25$. Open triangles are also with $\alpha = -1.25$, but for the broad bands U, B, V, R, I, and corrected to the AB_ν magnitude system.

Table 2 Luminosity function parameters of galaxies of different types and environments

Classification	N_g	α	M^*_R
early-type	180	–0.46 ± 0.17	–20.32 ± 0.17
late-type	128	–2.20 ± 0.24	–21.48 ± 0.83
dense-region	176	–0.65 ± 0.18	–20.25 ± 0.18
sparse-region	132	–2.00 ± 0.20	–23.19 ± 1.79

Some authors have calculated the LF of galaxy clusters. Lugger(1986) has measured the LFs of nine Abell clusters and found that the mean value of M^*_R is -22.66 with $\sigma_{M^*_R} = 0.66$. Oegerle et al. (1989) studied the LFs of eight rich Abell clusters and found $M^*_R = -22.49$ with $\sigma_{M^*_R} = 0.32$ (by taking $M_R = M_r - 0.6$). Our result of the $R-$band is $M^*_R = -20.85 \pm 0.22$ (with $\alpha = -1.25$). If we take $H_0 = 50\,\mathrm{km\,s^{-1}\,Mpc^{-1}}$, as was used in those papers, then $M^*_R = -22.20 \pm 0.22$. So, our result is in very good agreement with the previous results.

4 LUMINOSITY FUNCTIONS OF CLASSIFIED GALAXIES

4.1 The Morphological Dependence of LFs

As we know, early type galaxies tend to be redder than late type galaxies. This property can be used to classify early and late type galaxies. Following the method of Zhou et al. (2003), we regard galaxies with $m_c - m_h > 1.4$ as early type galaxies and the others as late type ones.

Based on this classification, we measured the R-band LFs of early and late type galaxies separately. The LFs are plotted in Figure 3, and the fitting parameters listed in Table 2. It is clear that the form of the Schechter function is still very good for both of them, but with significant quantitative differences between the two, as expected. The main difference is in the shape parameter, while the slope parameters are obviously different. For the early type galaxies, $\alpha_{\rm early}$ is -0.46 ± 0.17, and the profile tends to have a Gaussian shape, whereas for the late type galaxies, the value of $\alpha_{\rm late}$ is -2.20 ± 0.12, and the shape

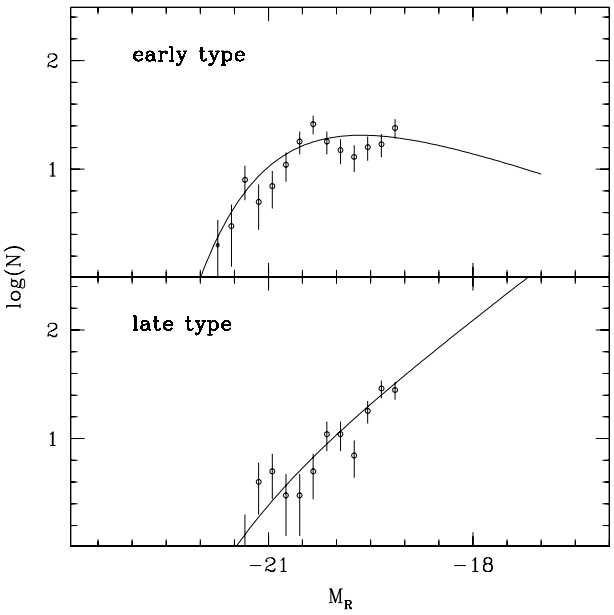

Fig. 3 LFs of early-type and late-type galaxies. The open circles represent the galaxy counts and the solid lines, the best-fitting LFs.

shows a power law behavior. Phenomenologically, this is because early type galaxies are mainly dominated by brighter galaxies, while late type galaxies have the power law distribution which is much more like the function due to the initial formation process of galaxies.

These results are similar to those reported by other authors. Using a sample of nearby optical galaxies (NOG), Marinoni et al. (1999) checked the difference of particular Hubble type LFs. They found a substantial dependence of the LF slope on the morphological type . The luminosity function is steeper in late type (S-Im) galaxies than in early type (E-S0) galaxies. More recently, Yagi et al. (2002) fitted individually Schechter function to early ($r^{1/4}$-like) and late (exponential-like) type galaxies of 10 nearby clusters, and their best-fitting Schechter function parameters are $M_R^* = -21.2$, $\alpha = -1.08$ for the early type galaxies and $M_R^* = -21.1$, $\alpha = -1.49$ for the late type galaxies. Shao et al. (2007) discussed the exponential-like galaxies of SDSS, and also found the slope of its LF to be obviously steeper than the other galaxies.

4.2 The Environment Dependence of LF

Galaxies in different environments are expected to have different formation histories: this is the well-known environmental effects, and the luminosity function of galaxies is an excellent tracer of this effect. Several previous studies have confirmed the difference of LFs between field galaxies and cluster galaxies, as well as between galaxies in dense and sparse regions of the cluster. Here we check whether the LFs of the member galaxies of Abell 566 are dependent on their environment.

We calculate first the local number density (μ, in units of deg^{-2}) of each member galaxy in the region that include the 10 nearest neighbors. Then all the member galaxies are separated according to their local density (μ) into two subsamples of about the same size. The LFs of the two subsamples are fitted by the Schechter function (Fig. 4). It is obvious that there is a distinct difference in the shape of the two LFs, with best-fitting shape parameters $\alpha_{\rm sparse} = -2.00 \pm 0.20$ and $\alpha_{\rm dense} = -0.65 \pm 0.18$ (Table 2). This trend is similar to the results reported by Beijersbergen et al. (2002). They studied the U-, B- and r-band luminosity functions of galaxies in the Coma cluster and drew a conclusion that the faint end slopes of all the three bands tend to be steeper from the center to the outskirt of the cluster. Meanwhile, Lopez-Cruz et al. (1997) and Paolillo et al. (2001) showed, on average, the slopes are steeper in the poorer than in the richer clusters. Our result further reinforces the evidence for environmental effects.

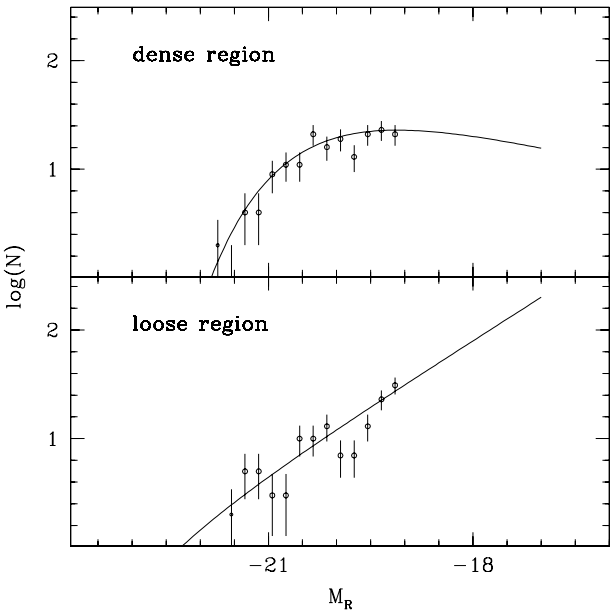

Fig. 4 Same as Fig. 3, but for galaxies in dense and sparse regions.

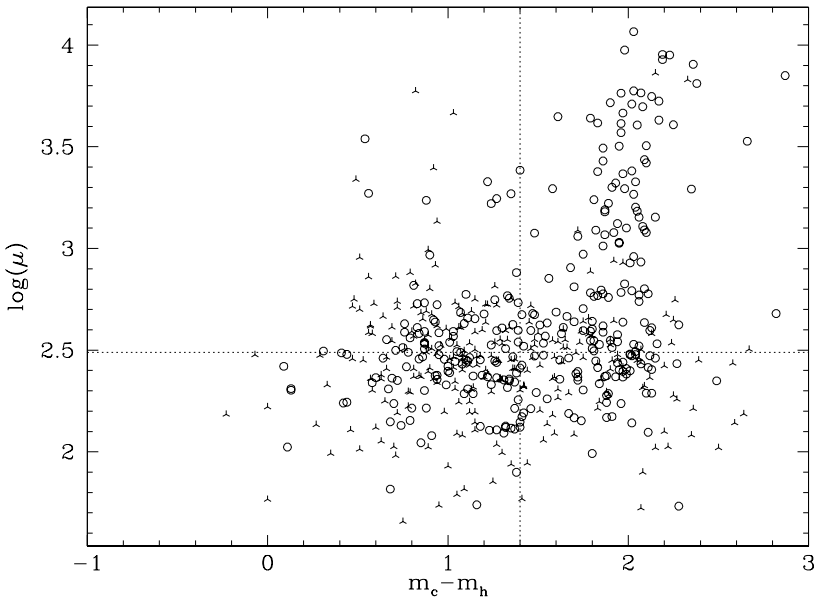

Fig. 5 Distribution of the Abell 566 galaxies in the 2-dimensional plot of color and local number density of galaxies. Each point represents a galaxy, with open circles for sample galaxies used in the fitting of LF and triangular stars for the rest galaxies.

4.3 Discussion

It is interesting that the environmental dependence of the LF is very similar to the morphological dependence: the LF of sparse region is similar to that of late type galaxies, and that of dense region is similar to

that of early type galaxies. This might seem to be a consequence of the density-morphology relationship that earlier type galaxies favor to stay in the denser regions, and vice versa, but this is not the case. After carefully comparing the galaxies of these subsamples, we found that the overlap between the 'sparse region' subsample and 'late type' subsample is 58%. This ratio is not very high, and it means there are quite a few of early type galaxies located in the sparse region. Also, the overlap between the 'dense region' subsample and 'early type' subsample is 70%, which means the early type galaxies are not the only occupiers of the dense region. Figure 5 is a plot of the galaxies in the 2-d 'space' of color and local number density, with dashed lines marking the subsample demarcation lines. So, the morphology-density relation is not the main reason for the similarity of the two dependences of the LF.

Intuitively, brighter galaxies, either giant ellipticals or early type spirals, are all located in the dense region, and late type spirals and galaxies in the sparse region are predominantly faint, with LF like the initial LF. This observation is more reasonably explained by the merger scenario in the cluster region: Originally, galaxies formed with the luminosity function (or mass function) with some power law liked profile. Then, in the dense regions, galaxies frequently interacted and merged to form larger galaxies, giving rise to more brighter galaxies. Also, in the dense region, dwarf galaxies are more easily captured by the massive galaxies, enhancing the brightness of the latter. On the other hand, similarity of the LFs for late-type galaxies and 'sparse region' galaxies can be explained by the fact that both have been free from strong interaction and so kept their original LF shape.

5 SUMMARY

We investigated the luminosity function of the galaxies in the cluster Abell 566. Using maximum-likelihood method, we measured the LFs for various wavebands, including 15 BATC intermediate bands and five broad bands (U, B, V, R and I). We found the LFs are well modelled by the Schechter function, in good agreement with previous studies.

Then, we classified the member galaxies in subsamples according to their colors and local number densities. We found significant evidence for morphological and environmental dependences of the LF. The LF has a steeper shape in late type than in early type galaxies. Also, the shape is steeper for galaxies in sparse than in dense regions.

After carefully comparing the subsamples, we argue that the density-morphology relationship is not the main reason of those dependences. Rather, they are better explained by the merger scenario. The interaction process invovled has seriously affected the properties of Abell 566, though it is still a young rich cluster.

Acknowledgements This research was supported by Grants 10273016 and 10333060 of the National Natural Science Foundation of China (NSFC) and Grant 2007CB815400 of the National Basic Research Program of China. The authors thank Prof. Qirong Yuan for his valuable advice.

References

Andreon S., 1998, A&A, 336, 98
Andreon S., Davoust E., Heim T., 1997, A&A, 323, 337
Beijersbergen M., Hoekstra H., van Dokkum P. et al., 2002, MNRAS, 329, 385
Bromley B. C., Press W. H., Lin H. et al., 1998, ApJ, 505, 25
Colless M., 1989, MNRAS, 237, 799
Dressler A., 1978, ApJ, 223, 765
Dresslar A., 1980, ApJ, 236, 351
Fan X., Burstein D., Chen J. S. et al., 1996, AJ, 112, 628
Jerjen H., Tamman G., 1997, A&A, 321, 713
Landolt A. U., 1983, AJ, 88, 439
Lumsden S. L., Collins C. A., Nichol R. C. et al., 1997, MNRAS, 290, 119
Lopez-Cruz O., Yee H. K. C., Brown J. P. et al., 1997, ApJ, 475, L97
Lugger P. M., 1986, ApJ, 303, 535
Marinoni C., Monaco P., Giuricin G. et al., 1999, ApJ, 521, 50
O'Donnell J., 1994, ApJ, 422, 158
Oegerle W. R., Hoessel J. G., 1989, AJ, 98, 1523

Oke J. B., Gunn J. E., 1983, ApJ, 266, 713
Paolillo M., Andreon S., Longo G. et al., 2001, A&A, 367, 59
Ramella M., Zamorani G., Zucca E. et al., 1999, A&A, 342, 1
Rauzy S., Adami C., Mazure A., 1998, A&A, 337, 31
Sandage A., Binggeli B., Tammann G. A., 1985, AJ, 90, 1759
Sandage A., Tammann G. A., Yahil A., 1979, ApJ, 232, 352
Schechter P., 1976, ApJ, 203, 297
Schlegel D. J., Finkbeiner D. P., Davis M., 1998, ApJ, 500, 525
Shao Z., Xiao Q., Shen S. et al., 2007, ApJ, 659, 1159
Struble M. F., Rood H. J., 1999, ApJS, 125, 35S
Trentham N., 1998, MNRAS, 294, 193
Valotto C. A., Nicotra M. A., Muriel H. et al., 1997, ApJ, 479, 90
Yagi M., Kashikawa N., Sekiguchi M. et al., 2002, AJ, 123, 87
Zhou X., Jiang Z. J., Xue S. J. et al., 2001, Chin. J. Astron. Astrophys. (ChJAA), 1, 372
Zhou X., Luo J., Sun X. P. et al., 2003, PASJ, 55, 891